DOI: 10.18727/0722-6691/5349

Mapping Galaxy Transformation with the MAGPI Survey

J. Trevor Mendel[1,2]
Katherine Harborne[3,2]
Claudia Lagos[3,2]
Emily Wisnioski[1,2]
and the MAGPI team

[1] Research School of Astronomy & Astrophysics, Australian National University, Canberra, Australia
[2] Australian Research Council Centre of Excellence for All Sky Astrophysics in 3 Dimensions
[3] International Centre for Radio Astronomy Research, The University of Western Australia, Perth, Australia

The Middle Ages Galaxy Properties with IFS (MAGPI) survey is an ongoing ESO Large Programme combining medium-deep Multi Unit Spectroscopic Explorer (MUSE) observations and an extensive library of simulated data to understand galaxy assembly over the past four billion years of cosmic time. Thanks to the combination of MUSE and the GALACSI adaptive optics system, MAGPI is delivering spatially resolved kinematic, star formation, and stellar population maps for hundreds of galaxies at intermediate redshift. By targeting galaxies across a range of environments, MAGPI will provide a unique perspective on the physical mechanisms responsible for transforming galaxy morphologies and kinematics at late cosmic times.

Galaxy transformation during the assembly epoch

Current models for the formation of massive galaxies (> 10^{11} solar masses) suggest two distinct evolutionary phases. At early times their growth is expected to be driven by rapid *in-situ* star formation fed by the accretion of gas from the cosmic web. The relative balance of accretion, star formation, and feedback during this first 'formation' phase leads to a tight linear relation between stellar mass and star formation rate for normal star-forming galaxies. Galaxies appear to maintain a relatively high star formation duty cycle (30–70%) until their star formation is quenched, either through the removal of a suitable gas reservoir or suppression of gas cooling (for example, Man & Belli, 2018). This quenching process, which marks the transition to the second phase of galaxy formation, leads to the build-up of a massive, passive galaxy population whose evolution is then dominated by the assembly of stellar mass formed *ex-situ* through mergers.

Spatially and spectrally resolved observations over the past several decades have sharpened our view of the early formation phase. Among other things, deep observations with the Very Large Telescope's (VLT) Spectrograph for INtegral Field Observations in the Near Infrared (SINFONI), the *K*-band Multi Object Spectrograph (KMOS), and the Atacama Large Millimeter/submillimeter Array (ALMA) during the epoch of peak star formation at z = 2–3 have highlighted that most stars appear to form in turbulent, gas rich, marginally stable discs (Förster Schreiber et al., 2009; Wisnioski et al., 2015; Stott et al., 2016; Liu et al., 2019). These kinematic results are supported by JWST imaging in the rest-frame near-infrared that highlights an abundance of disc galaxies in the early Universe (Ferreira et al., 2022, 2023; Kartaltepe et al., 2023; Nelson et al., 2023). Taken together, these observational results are consistent with the early stages of massive galaxy formation described previously, i.e., in which growth is dominated by *in-situ* star formation.

At late times, as the cosmological accretion rate falls, the dominant pathway for galaxy growth is expected to transition from *in-situ* star formation to the assembly of stars formed *ex-situ*. As well as providing a pathway for continued growth in the absence of ongoing star formation, galaxy-galaxy interactions are expected to transform early disc-dominated systems into the diverse range of morphologies mapped by the Hubble sequence in the nearby Universe. Simulations predict that repeated minor-merging in particular can account for the lack of massive, compact, and rotationally supported galaxies seen locally. These predictions are borne out by observations that suggest massive galaxies today are a factor of 3–5 larger and have substantially lower angular momentum than their expected progenitors at $z > 1$ (for example, Belli, Newman & Ellis, 2014; Bezanson et al., 2018). Detailed investigations of the stellar populations in nearby galaxies — especially radial profiles of age, metallicity, and alpha-element abundance — further support a picture in which the accretion of low-mass, gas-poor satellites is the primary driver of massive galaxy evolution during this assembly epoch.

While the outcomes of the assembly process are made manifest in the diversity of galaxies we observe in the nearby Universe, understanding when and how this diversity developed is challenging. Observations of nearby galaxies using integral field spectrographs (IFS) leverage a combination of resolved kinematics and stellar populations to untangle this story using archaeological methods. Kinematic features and metallicity gradients of stars and gas can reveal hints of the evolutionary path for an individual galaxy (Taylor & Kobayashi, 2017; Tissera et al., 2018; Martig et al., 2021), the details of which are further expected to depend on the properties of its host environment (Foster et al., 2021). It is therefore crucial to study massive galaxies in a resolved manner at different cosmic times and across a range of different environments.

It is with this context in mind that we have undertaken the Middle Ages Galaxy Properties with IFS (MAGPI) survey, which represents one of the first systematic studies of resolved stellar and gas properties at intermediate lookback times. Unlike previous surveys, MAGPI utilises the unique capabilities of the Multi Unit Spectroscopic Explorer (MUSE) and the Adaptive Optics Facility (AOF) of the VLT to obtain data with a physical resolution comparable to that of local IFS surveys such as Mapping Nearby Galaxies at APO (MaNGA; Bundy et al., 2015) and the Sydney-AAO Multi-object Integral field spectrograph (SAMI) survey (Bryant et al., 2015). These data therefore enable a unique comparison of resolved galaxy properties across a range of environments and lookback times.

Data

The MAGPI survey comprises two parts. The first is a set of medium-deep IFS observations using MUSE and the GALACSI adaptive optics system to probe massive galaxies and their

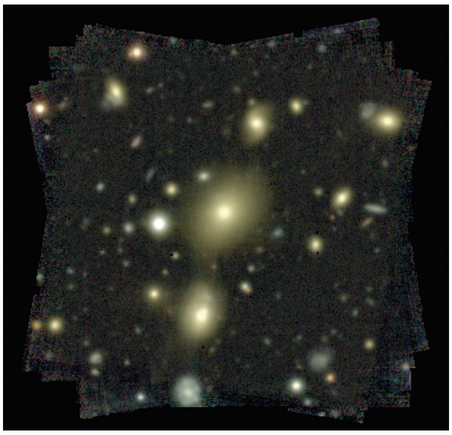

Figure 1. Mock Sloan Digital Sky Survey (SDSS) *gri*-band image computed using MUSE data for the MAGPI 1501 field.

environments at $z \sim 0.3$. The second is a suite of mock IFS data tailored to match these observations and facilitate a detailed comparison with state-of-the-art cosmological simulations.

The MAGPI MUSE survey

The observational component of MAGPI leverages the wide field of view and excellent image quality delivered by GALACSI+MUSE to survey 56 independent fields. Each field is centred on a massive ($M_\star > 7 \times 10^{10}$ solar masses) 'primary' galaxy at $0.25 < z < 0.35$ and its surrounding environment. All observations are carried out using MUSE in the WFM-AO mode. Potential targets were first identified within the Galaxy And Mass Assembly (GAMA) survey (Driver et al., 2011) G12, G15 and G23 fields to span a range of environments and galaxy colours, with the final selection driven by the availability of suitably bright tip-tilt stars from Gaia DR2. As of December 2023, observations have been completed for 49 of the 56 target fields.

The average exposure time for any given section of the ~ 1-arcmin^2 MUSE field is four hours, and data reduction for the survey is carried out using the ESO MUSE data reduction pipeline (Weilbacher et al., 2020). The final reduced and calibrated data cubes are photometrically complete down to $i_{AB} \sim 26$ mag (3σ), and spectroscopically complete down to $i_{AB} \sim 22$ mag.

The median *i*-band image quality is 0.55 arcseconds, assessed either using point sources available in a subset of the fields or via reconstruction of the adaptive optics point spread function using MUSE-PSFR (Fusco et al., 2020). An example of the reduced data for one field, MAGPI 1501, is shown in Figure 1.

Given the physical extent of the MUSE field of view projected at $z \sim 0.3$ (~ 270 kpc), each MAGPI field includes not only the galaxy of interest, but a host of satellite and background galaxies that facilitate a range of additional science. Sources in each field are identified and catalogued using ProFound (Robotham et al., 2018) based on a series of white-light and narrow-band images, and subsequently have redshifts manually assigned using the redshifting software package MARZ (Hinton et al., 2016). Across the current survey this process has identified ~ 400 low-mass satellite galaxies in our redshift range of interest ($0.25 < z < 0.35$) and another > 1200 objects at $z > 0.4$, all with secure redshifts.

The MAGPI theory survey

From the outset it was clear that disentangling the various internal and external processes driving galaxy transformation at late times would be challenging given observational data alone. For this reason, a key deliverable of MAGPI is the associated theory survey, in which mock MUSE observations have been constructed for a growing number of large, cosmological hydrodynamical simulations. Currently this includes Evolution and Assembly of GaLaxies and their Environments (EAGLE; Schaye et al., 2015; Crain et al., 2015), IllustrisTNG (Pillepich et al., 2018; Nelson et al., 2019), Magneticum (Teklu et al., 2015; Dolag, Komatsu & Sunyaev, 2016), and HorizonAGN (Dubois et al., 2016).

Current cosmological models are extremely complex, with a variety of recipes to account for effects below the resolvable scales in the model. An example of this complexity for the suite of simulations currently included in the MAGPI theory survey is demonstrated in Figure 2. While all simulations include the key ingredients necessary for galaxy formation and evolution — gravity, gas cooling, star formation, stellar and black hole feedback etc. — the specific recipe for each ingredient used can vary substantially. All of these elements are important for reproducing ensemble properties of the galaxy population (for example, stellar

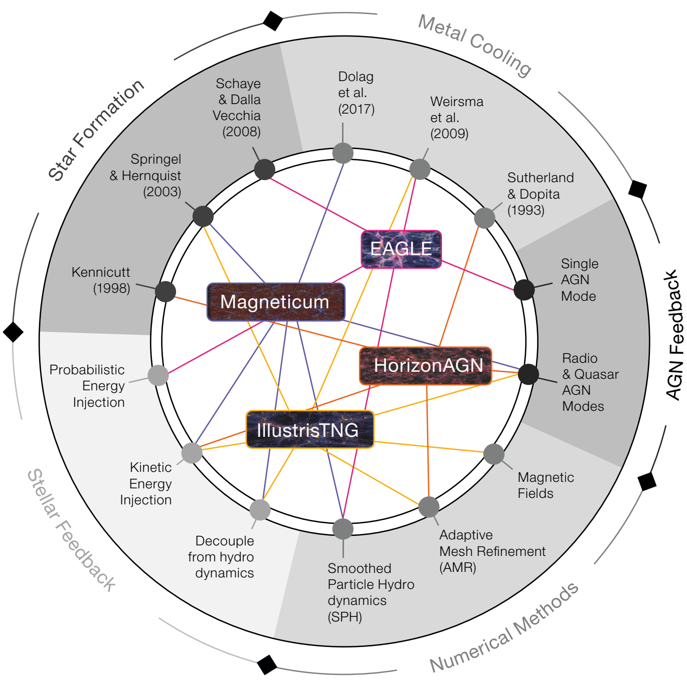

Figure 2. Demonstrating the basic ingredients for a cosmological model of galaxy formation and evolution. The models explored by the MAGPI Theory Stream are shown in the centre. Each model has links to the specific recipe used for each necessary ingredient. This makes clear the complexity of comparing different models and justifies the necessity of comparable data products. Figure adapted from Harborne et al. (in preparation).

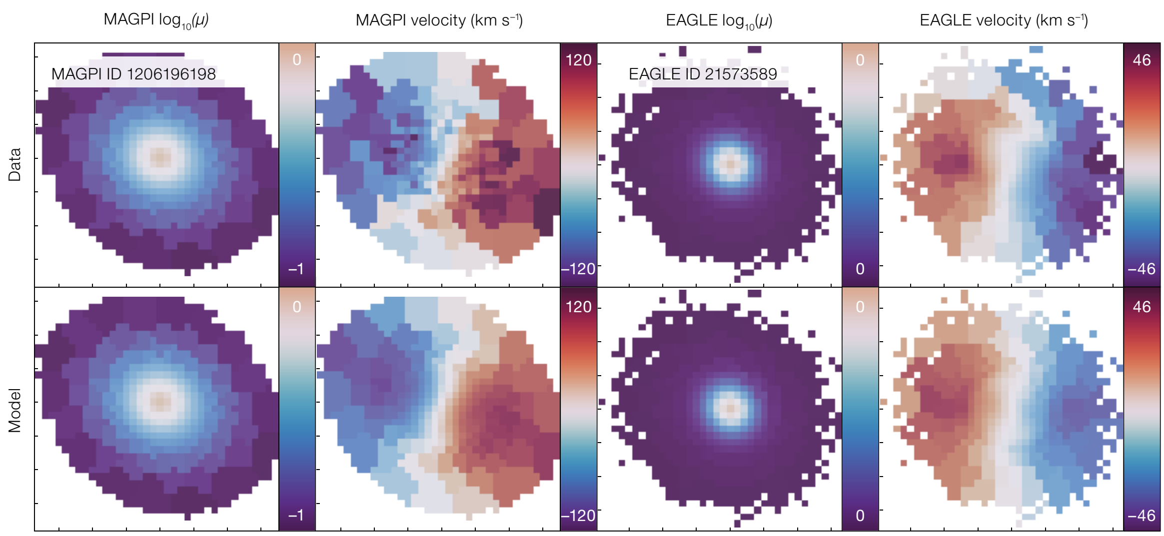

Figure 3. Two-dimensional surface brightness (first and third columns) and velocity (second and fourth columns) maps for one MAGPI galaxy (on the left) and one EAGLE galaxy (on the right). The top rows show data obtained from MUSE and analogous data from the EAGLE simulation produced using SimSpin. The bottom row shows the reconstruction of these data using DYNAMITE. Figure adapted from Derkenne et al. (in preparation) and Santucci et al. (in preparation).

mass, size etc.), but disentangling the effects of these sub-grid recipes and their relation to our observations requires a like-for-like comparison.

In order to build a comparable theory sample we have been using the open-source package SimSpin (Harborne, Power & Robotham, 2020; Harborne et al., 2023) to generate mock MUSE observations of simulated galaxies. This code is designed to be agnostic to the type of simulation input, including support for many flavours of different hydrodynamical models and various numerical methods; it is also easily configured to mimic a range of different instruments including MUSE, SAMI, and the MaNGA instrument. Output mock observations can be produced in the format of spectral data cubes, such that reduction pipelines and kinematic line-fitting software can be optimised and tested. SimSpin can also produce kinematic maps comparable to those output by our data analysis pipeline, but without the fitting procedure. This enables fast iteration across a range of projection angles and seeing conditions, for investigation into specific features and their evolution throughout cosmic time.

Key science

MAGPI data allow us to map kinematics and stellar populations across a range of galaxy spatial scales and environments, and a full outline of the science goals for the survey can be found in Foster et al. (2021). Here we highlight recent progress in several areas which seek to connect these data to observations at both low and high redshift.

Stellar dynamics

Stellar kinematics are powerful tracers of galaxy formation and evolution, as they encode the full history of processes impacting galaxy growth over cosmic time. Early results combining MAGPI with SAMI at $z = 0$ and the Large Early Galaxy Astrophysics Census (LEGA-C; van der Wel et al., 2016) at $z \sim 0.8$ have already demonstrated significant evolution of high-order stellar kinematic parameters (in particular h_4), confirming the importance of galaxy mergers to the evolution of massive galaxies (D'Eugenio et al., 2023a,b). The broad range of environments probed by MAGPI have also been used to show that environment plays a secondary but significant role moderating the internal mass distribution of galaxies at intermediate cosmic times (Derkenne et al., 2023).

Going beyond single parameter indicators of stellar kinematics can help to further isolate the relative importance of internal and external processes, where *in-situ* star formation and mergers/accretion are expected to influence the balance of hot and cold orbits in different ways. Within MAGPI we are using DYnamics, Age, and Metallicity Indicators Tracing Evolution (DYNAMITE; Jethwa et al., 2020) to reconstruct data from the MAGPI MUSE and theory surveys. DYNAMITE is a next-generation implementation of the Schwarzschild orbit superposition method, which uses a weighted library of numerically integrated stellar orbits to reproduce observables such as surface brightness and kinematic moments (for example, v, σ, h_3, h_4).

Figure 3 shows an example of DYNAMITE applied to both MAGPI and EAGLE galaxy data, illustrating its ability to reproduce details of MUSE observations (in this case surface brightness and velocity) even at $z = 0.3$. The value of this analysis is twofold: first, it facilitates an assessment of the orbit reconstruction, and especially its dependence on spatial and spectral resolution, through comparison with the simulated particle data; and second, it allows a direct comparison with observations, such that the orbital distribution in simulations can be used to study the origin of different kinematic components in the data.

Stellar populations

Where kinematics help us to understand details of the assembly process, stellar populations provide a view of when and where stars form. MAGPI spectra are sufficiently deep that they facilitate mapping

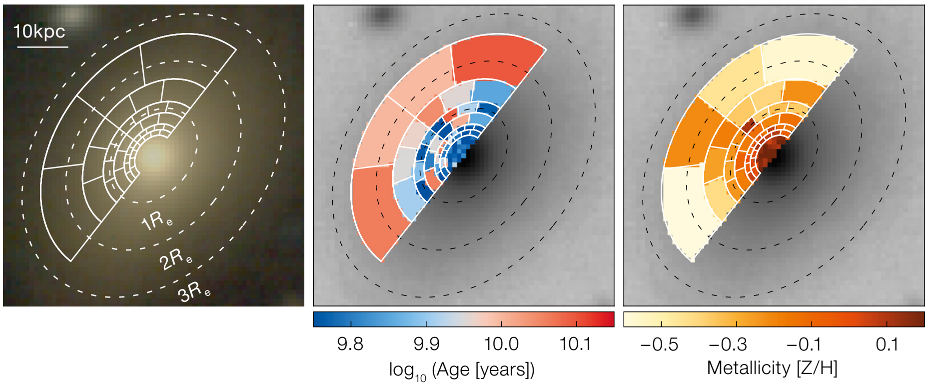

Figure 4. Example stellar population measurements derived for the primary galaxy in MAGPI 1501 (i.e., Figure 1). Left to right, the panels show the mock *gri*-band image, light-weighted stellar age, and light-weighted stellar metallicity in annular and azimuthal bins as indicated. Dotted lines mark 1, 2 and 3 half-light radii (R_e) as indicated. Figure adapted from Mendel et al. (in preparation).

key stellar population parameters such as mean metallicity and mean stellar age out as far as two to three half-light radii when binned. An example for one of the MAGPI central galaxies is shown in Figure 4, where the stellar age and metallicity, [*Z/H*], are traced out to about two half-light radii with individual bins reaching a signal-to-noise in the continuum of more than 20.

The value of these measurements is more clearly illustrated in Figure 5, where we compare MAGPI data against stellar population profiles derived for MaNGA galaxies by Lu et al. (2023). We find that the metallicity gradients derived for MAGPI are entirely consistent with MaNGA galaxies of a similar mass; however the derived age gradients are substantially flatter, particularly in the outskirts. The interpretation of falling age gradients by Lu et al. (2023) is that of an increased contribution from a young stellar disc outside the central bulge region, suggesting that MAGPI galaxies may lack a comparable disc-like component.

Star formation

Despite the majority of MAGPI primary galaxies being relatively gas poor, a number of galaxies across the survey host substantial, extended gas discs whose properties can be used to understand recent gas accretion and the role of environment in modulating star formation activity. Figure 6 shows the distribution of MAGPI galaxies in terms of star formation rate (SFR) and stellar mass, where the sample has been limited to only those objects in the range of $0.25 < z < 0.42$ with robust SFR estimates. This Figure emphasises the power of MAGPI data for studying a broad range of galaxies, where in this case we trace the global SFR–mass relation over about five orders of magnitude in stellar mass.

In addition to these integrated measurements, many star-forming galaxies are resolved by the MAGPI point spread function and can be used to study radial profiles of star formation, in many cases out to two or three effective radii. A detailed comparison of these data with SFR profiles from MaNGA will be presented in Mun et al. (submitted to MNRAS).

The distant Universe

In addition to our primary targets, MAGPI data reveal many background sources which are identified using strong emission and absorption features from the far-UV, for example Lyα to [OII]. The combination

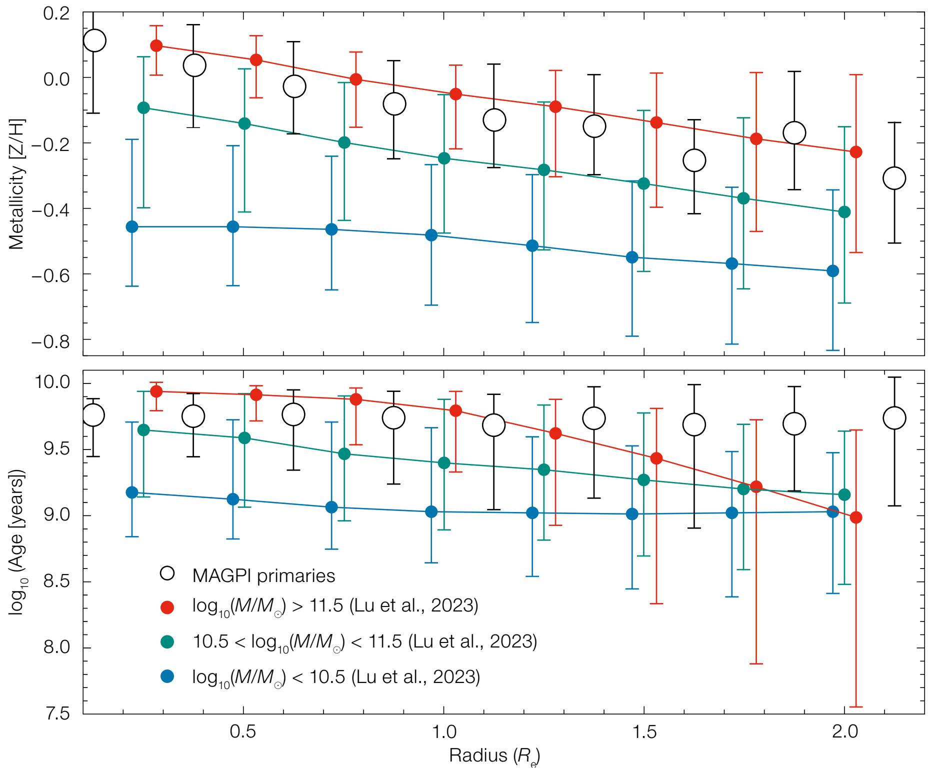

Figure 5. Comparison of metallicity (top) and age (bottom) profiles between MAGPI primary galaxies and comparable galaxies in MaNGA as derived by Lu et al. (2023), demonstrating the large spatial coverage of MAGPI. Figure adapted from Mendel et al. (in preparation).

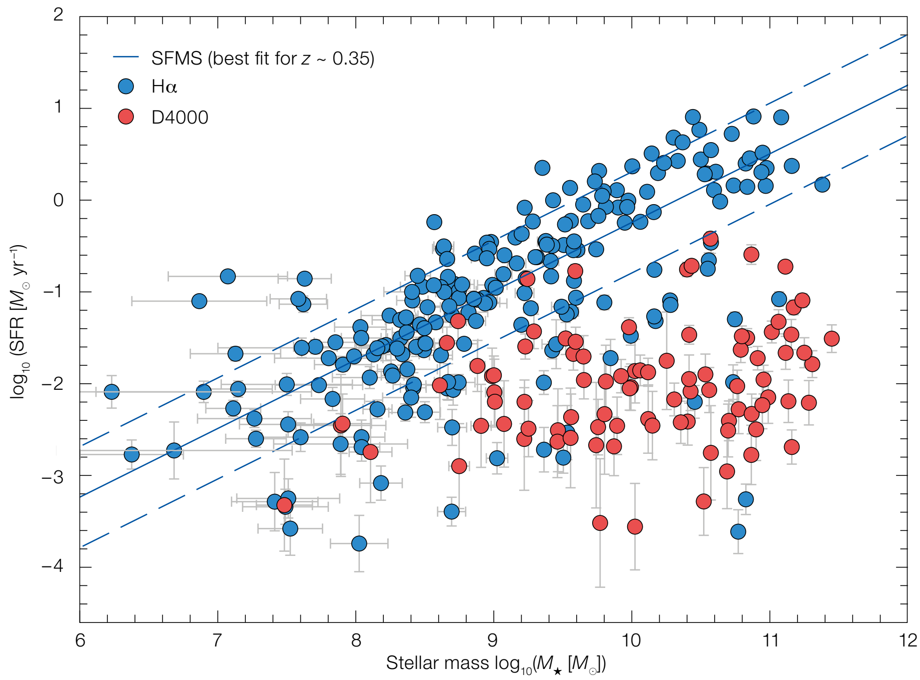

Figure 6. Star Formation Rate (SFR) as a function of stellar mass for current MAGPI fields. The blue line shows a best fit for the star formation main sequence (SFMS) derived from Hα data. This figure is adapted from Mun et al. (submitted to MNRAS).

of wide area (56 arcmin^2) and intermediate exposure time (4 hours) mean MAGPI is ideally suited to the discovery of rare, bright targets compared to other MUSE surveys (for example MUSE deep and MUSE-Wide), with a reduction in cosmic variance due to the spatially disjoint nature of the survey footprint. This has already been realised with the discovery of three rare double-peaked Lyα emitters at $2.9 < z < 4.8$ exhibiting strong blue-peak emission (Mukherjee et al., 2024). Two of these three are extended sources covering areas of 25 × 26 kpc ($z = 2.9$) and 19 × 28 kpc ($z = 3.6$), with the strongest contribution to the blue emission from bright cores associated with the sources. In contrast, the third blue-peak Lyα emitter, at $z \sim 4.8$, is a compact system and stands as the highest-redshift strong blue-peak emitter ever detected.

Galaxies with strong blue-peak emission are unique systems providing insight into the scattering of Lyα photons by neutral hydrogen. Lyα lines with a stronger blue peak than the red peak usually imply inflows of circumgalactic medium gas along the line of sight during the accretion phase (for example, Ao et al., 2020; Blaizot et al., 2023). In this context, the galaxies discovered in MAGPI suggest inflowing gas systems or edge-on morphologies. Recent cosmological zoom-in simulations (Blaizot et al., 2023) predict < 20% of double-peaked Lyα emitters should have a dominant blue peak, which is consistent with the numbers presented by Mukherjee et al. (2024). These three systems are a part of a larger campaign to catalogue Lyα emitters and absorbers with MAGPI fields — currently 360 new sources across 35 MAGPI fields.

Outlook

MAGPI is a first step towards building large, spatially and spectrally resolved samples of stellar kinematics outside the nearby Universe. Future ESO facilities like the MCAO Assisted Visible Imager and Spectrograph (MAVIS) on the VLT and the High Angular Resolution Monolithic Optical and Near-infrared Integral field spectrograph (HARMONI) on ESO's Extremely Large Telescope will enable us to push such resolved lookback studies even farther, dramatically improving our ability to confront complex cosmological simulations with equally detailed observational constraints.

Combining these resolved stellar and (ionised) gas data with atomic and molecular gas measurements is an obvious next step towards understanding the full baryon cycle in galaxies at these intermediate redshifts. Such observations are already within reach of ALMA and the Northern Extended Millimeter Array (NOEMA), and will be a priority for the Square Kilometre Array (SKA) and SKA pathfinder surveys.

Acknowledgements

We would like to thank the ESO staff on Paranal for their substantial and ongoing support throughout the MAGPI observing programme.

References

Ao, Y. et al. 2020, Nat. Astron., 4, 670
Belli, S., Newman, A. B. & Ellis, R. S. 2014, ApJ, 783, 117
Bezanson, R. et al. 2018, ApJ, 858, 60
Blaizot, J. et al. 2023, MNRAS, 523, 3749
Bryant, J. J. et al. 2015, MNRAS, 447, 2857
Bundy, K. et al. 2015, ApJ, 798, 7
Crain, R. A. et al. 2015, MNRAS, 450, 1937
Derkenne, C. et al. 2023, MNRAS, 522, 3602
D'Eugenio, F. et al. 2023a, MNRAS, 525, 2765
D'Eugenio, F. et al. 2023b, MNRAS, 525, 2789
Dolag, K., Komatsu, E. & Sunyaev, R. 2016, MNRAS, 463, 1797
Driver, S. P. et al. 2011, MNRAS, 413, 971
Dubois, Y. et al. 2016, MNRAS, 463, 3948
Ferreira, L. et al. 2022, ApJL, 983, L2
Ferreira, L. et al. 2023, ApJ, 955, 94
Förster Schreiber, N. M. et al. 2009, ApJ, 706, 1364
Foster, C. et al. 2021, PASA, 38, 31
Fusco, T. et al. 2020, A&A, 635, A208
Hinton, S. R. et al. 2016, A&C, 15, 61
Harborne, K. E., Power, C. & Robotham, A. S. G. 2020, PASA, 37, 16
Harborne, K. E. et al. 2023, PASA, 40, 48
Jethwa, P. et al. 2020, ASCL, 2011.007
Kartaltepe, J. S. et al. 2023, ApJL, 946, L15
Liu, D. et al. 2019, ApJ, 887, 235
Lu, S. et al. 2023, MNRAS, 526, 1022
Man, A. & Belli, S. 2018, Nat. Astron., 2, 695
Martig, M. et al. 2021, MNRAS, 508, 2458
Mukherjee, T. et al. 2024, A&A Lett., in press, arXiv:2311.07019
Nelson, D. et al. 2019, ComAC, 6, 2
Nelson, E. J. et al. 2023, ApJL, 948, L18
Pillepich, A. et al. 2018, MNRAS, 473, 4077
Robotham, A. S. G. et al. 2018, MNRAS, 476, 3137
Schaye, J. et al. 2015, MNRAS, 446, 521
Stott, J. P. et al. 2016, MNRAS, 457, 1888
Taylor, P. & Kobayashi, C. 2017, MNRAS, 471, 3856
Teklu, A. F. et al. 2015, ApJ, 812, 29
Tissera, P. B. et al. 2018, MNRAS, 473, 1656
van der Wel, A. et al. 2016, ApJS, 223, 29
Wisnioski, E. et al. 2015, ApJ, 799, 209
Weilbacher, P. M. et al. 2020, A&A, 641, A28